EPJ Web of Conferences **67**, 02101 (2014)
DOI: 10.1051/epjconf/20146702101

Characterization of the cavitating flow in converging-diverging nozzle based on experimental investigations

Pavel Rudolf[1,a], Martin Hudec[1] , Milan Gríger[1]and David Štefan[1]

[1]Brno University of Technology, Faculty of Mechanical Engineering, V. Kaplan Department of Fluids Engineering, Technická 2896/2, 61669 Brno, Czech Republic

Abstract. Cavitation phenomena occuring in converging-diverging nozzle (Venturi tube) are described in the paper. A closed test circuit with possibility to control both flow rate and static pressure level were used. Loss coefficient was evaluated for different sigma numbers resulting in full „static" characterization of the nozzle. Visualizations of the cavitation pattern development were acquired and matched with evolution of the loss coefficient. Three cavitation regimes are described: partial cavitation, fully developed cavitation, supercavitation.

1 Introduction

Cavitation occurs in liquids when the local value of the absolute pressure reaches so called saturated vapor pressure. Discontinuities filled with vapor can have form of bubbles, sheets, clouds, cavitating vortices. Appearance and structure of the cavitation strongly depends on hydrodynamic characteristics of the flow (e.g. static pressure level) and geometry of the flow domain. Developed cavitating structures block the flow resulting in substantial increase of hydraulic losses. Furthermore, presence of compliant cavitating phase, which experiences severe condensation/evaporation cycles, interfers dynamics of the flow. Existence of cavitation is a limiting factor for operation of all hydraulic machines and devices, e.g. hydraulic turbines, pumps, valves. On the other hand cavitation can be exploited for enhancing of chemical reactions (sonochemistry) or cleaning processes.

Fully developed cavitation can lead to so called supercavitation, when the vapor region extends the body dimensions and propagates quite far downstream. Supercavitation is well known in ship propellers or around underwater projectiles (torpedo) and vehicles. Supercavitation phenomenon is mostly studied for case of external hydrodynamics when the vapor filled bubble closes behind the body subjected to fast flowing liquid stream. It is less common to observe supercavitation within pipes.

Present contribution focuses on cavitation appearance in converging-diverging (CD) nozzle (also known as Venturi tube). It is probably the simpliest device for observation of hydrodynamic cavitation. Yet it enables to study cavitation in its full complexity: cavitation inception, hydraulic losses induced by presence of cavitation, cavitation within separated boundary layers, transition from sheet to cloud cavitation, pressure pulsations induced by cavitation collapse, supercavitation phenomenon, etc.

Older investigations of Venturi tubes, aimed especially on erosion testing, are found in classical books of Knapp [1] and Hammitt [2]. Venturi tubes are also applied in hydraulic cavitation tunnels to study water quality, i.e. nuclei content [3]. Converging-diverging nozzle has also become a popular testcase for development of cavitation models included in CFD softwares [4-6] or for visualization of cavitation patterns by non-intrusive techniques [7, 8]. However these experiments are based on asymmetric planar CD nozzle with rectangular cross-section. This geometrical configuration does not enable boundary layer separation in form of vortex ring development and also supercavitation regime is not documented. Present paper is directed toward CD nozzle with circular cross-section, which is more common in pipeline systems.

2 Experimental circuit

Closed hydraulic test circuit was used to study cavitation in CD nozzle. Water is supplied by pump (Lowara) controlled via frequency converter (Frenic-Multi), which ensures comfortable adjustment of flow rate over relatively wide range. Level of static pressure within circuit is modified by vacuum pump or pressurized air injection above the water level in pressure vessel. Combination of flow rate and static pressure control enables to operate the circuit from no cavitation regime to full supercavitation. CD nozzle is manufactured by CNC

[a] Corresponding author: rudolf@fme.vutbr.cz

machining and polishing from cast plexiglass to allow visualization. Edges between regions of changing cross-section are made sharp to clearly define separation points. Static pressures were recorded in four stations. Common pressure transducers based on strain gauge principle (DMP331, BD Sensors, accuracy ±0.25% of the range) were used together with ultrafast piezoelectric transducers (701A, Kistler, accuracy ±0.3% of the range). Flow rate was measured by induction flowmeter (MQI99, ELA, accuracy ±0.5% of the range). Temperature data were acquired by resistance thermometer (HSO-502 1A2L, HIT, accuracy ±0.1% of the range). Electric signals from all transducers and sensors are collected via data acquisition system NI9184 (National Instruments). Measurements were conducted in LabVIEW environment.

Photos of cavitation patterns were made by digital camera Nikon D300, two halogen lamps were used as light sources, each of them with 500 W output.

It should be noted that prior measurements the circuit was operated for at least 45 minutes in maximum accessible negative pressure to minimize amount of gas content. However no measurement of gas content or nuclei number was performed.

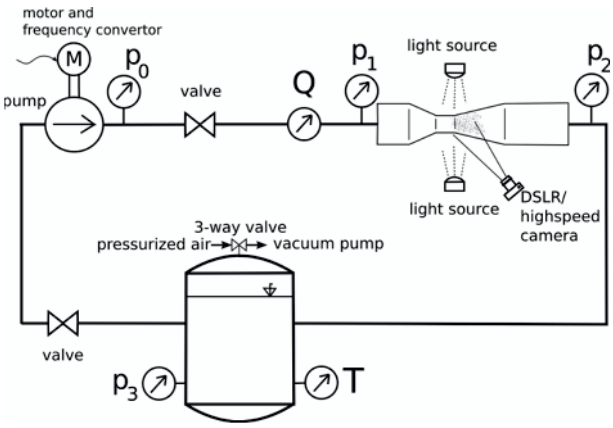

Figure 1. Scheme of the hydraulic circuit

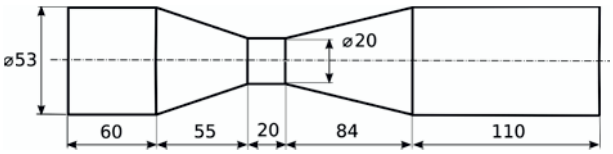

Figure 2. Converging - diverging nozzle layout

3 Measurements

Cavitation number is usually used to characterize the state of the cavitating flow. Though, the definitions of cavitation number vary significantly. Definition based on the downstream pressure and velocity in the throat of the CD nozzle is used throughout this paper:

$$\sigma = \frac{p_2 - p_{vapor}}{\rho \frac{v_{throat}^2}{2}} \quad (1)$$

where vapour pressure depends on water temperature according to modified Clausius-Clapeyron equation:

$$p_{vapor} = 100 \cdot e^{53.67957 - \frac{6743.69}{T} - 4.8451 \cdot lnT} \quad (2)$$

Using the downstream pressure should emphasize that the pressure vessel close to sensor p_2 controls the static pressure level in the circuit. Alternatively different definition was also applied, which is often used in study of cavitating valves [9, 11]:

$$\mathrm{z} = \frac{p_1 - p_2}{p_1 - p_{\mathrm{vapor}}} \quad (3)$$

Finally a reciprocated value of z is used, which is consistent to cavitation index definition by [10, 11].

$$z^{-1} = \frac{1}{z} = \frac{p_1 - p_{\mathrm{vapor}}}{p_1 - p_2} \quad (4)$$

The effect of cavitation on energy dissipation is studied using loss coefficient of the CD nozzle:

$$\zeta = \frac{p_1 - p_2}{\rho \frac{v_{throat}^2}{2}} \quad (5)$$

Again alternatively a different measure of the hydraulic losses is applied, which is used in the valve design and testing – flow factor K_v:

$$K_v = 36000 \cdot Q \sqrt{\frac{\rho}{p_1 - p_2}} \quad (6)$$

The goal of using different coefficients for characterization of the cavitation and energy loss respectively is to find sensitive tool to distinguish among the different cavitation regimes. The comparison is done for data obtained with vessel open to atmospheric pressure, only flow rate is controlled. However, results plotted in figures 3, 4, 5 do not indicate any better ability of the alternative definitions above the classical cavitation number σ and loss coefficient ζ. Moreover ζ is nondimensional ($[K_v] = m^3/hour$), hence more suitable in experimental fluid mechanics to make comparisons between different flow situations or geometrical configurations.

The typical evolution of the loss coefficient is depicted in figure 6, again for case of vessel open to atmosphere. Losses remain the same with decreasing cavitation number until the point close to visual cavitation inception. By visual cavitation inception is understood the situation, when first cavitation bubble discernible by naked eye appears.

Slight loss decrease is apparent on the zoomed view of the graph, which resembles efficiency increase of hydraulic machines just before the onset of cavitation.

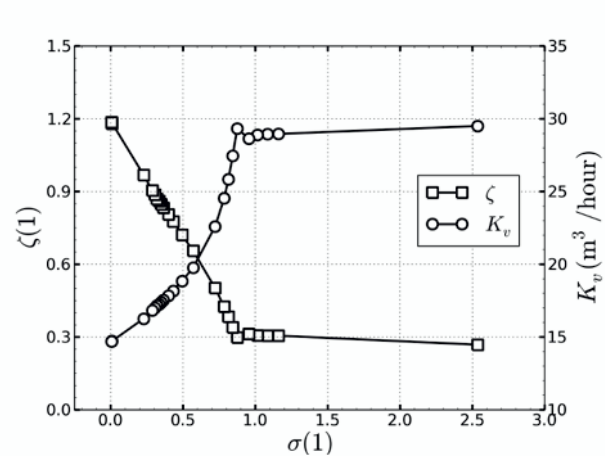

Figure 3. Loss coefficient and flow factor vs. cavitation number – circuit open to atmosphere

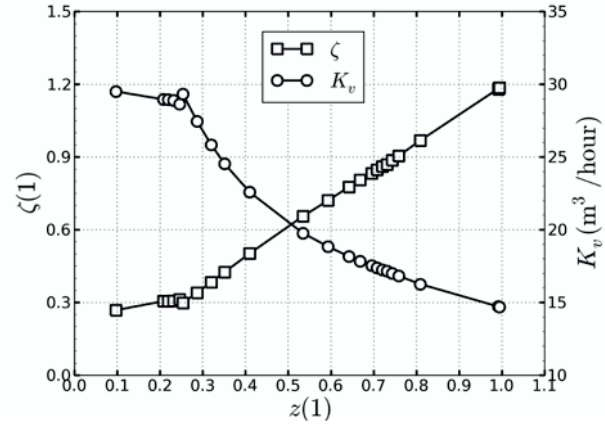

Figure 4. Loss coefficient and flow factor vs. modified cavitation number – circuit open to atmosphere

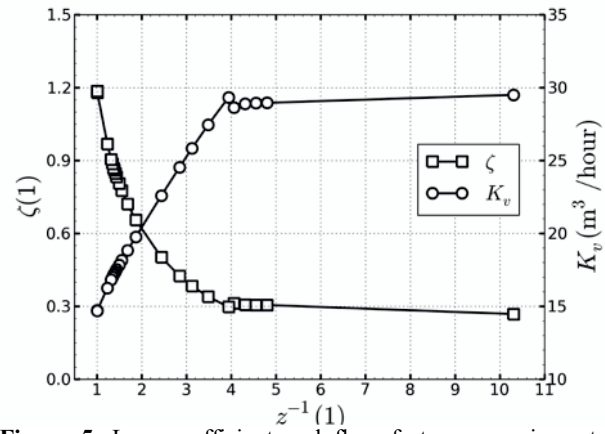

Figure 5. Loss coefficient and flow factor vs. reciprocated value of the modified cavitation number – circuit open to atmosphere

This behaviour is usually explained by inception of bubbles in the near wall region and thereby reduced friction. Further pressure decrease leads to cavitation bubble expansion and origin of sheet cavitation, resulting in blockage effect and energy loss growth. Further development of loss coefficient is almost linear in $\zeta - \sigma$ coordinates for all other regimes of cavitating flow. When developed supercavitation is reached all measured data collapse into a single point. This fact is due to placing of pressure sensor p_2 in the supercavitating region, i.e. this sensor measures vapour pressure, which corresponds to cavitation number equal to zero. Further decrease of cavitation number was not possible due to limited flow capacity of the circuit.

Another series of measurements was done keeping constant flow rate and varying the overall static pressure level either by pressurized air or vacuum pump. Obviously both approaches should be equivalent. The graphs do not span the same range of cavitation numbers, because of the limitations in circuit capacity, vacuum pump performance and tightness of the circuit. Nevertheless figure 14, which depicts points of visual cavitation inception and transition to supercavitation, shows relatively good agreement among all sets of measurements. Similar behavior can be shown for points defining transition from partial cavitation to fully developed cavitation. It should be noted that repeatability of cavitation experiments is very problematic, because of changing parameters of the liquid (nuclei number, gas content, purity). Differentiation among the regimes is also exposed to error in observation and interpretation of the photos. Future research will focus on definition of the regimes based on amplitude of pressure pulsations.

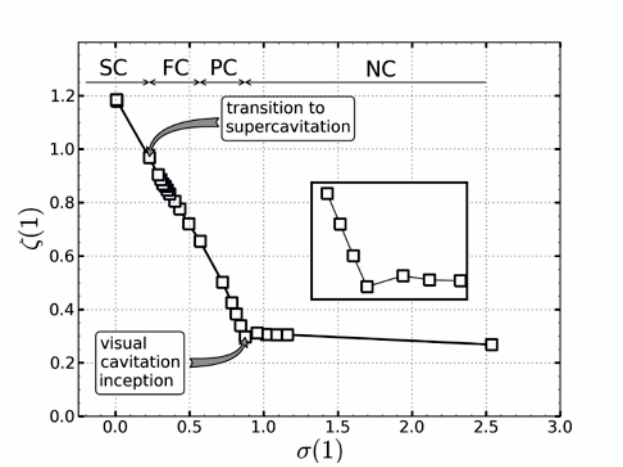

Figure 6. Cavitation regimes for full range of cavitation numbers – circuit open to atmosphere (NC – no cavitation, PC – partial cavitation, FC- full cavitation, SC – supercavitation)

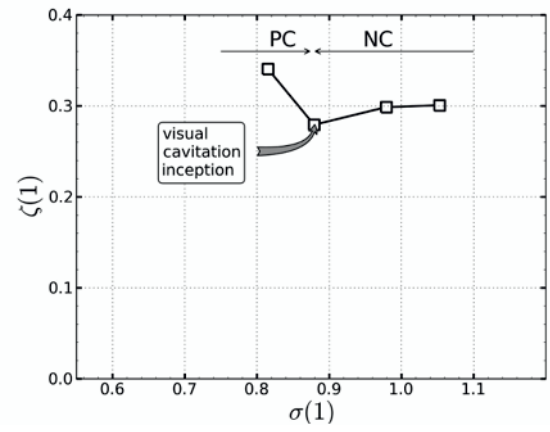

Figure 7. Q = const =4 l/s (NC – no cavitation, PC – partial cavitation)

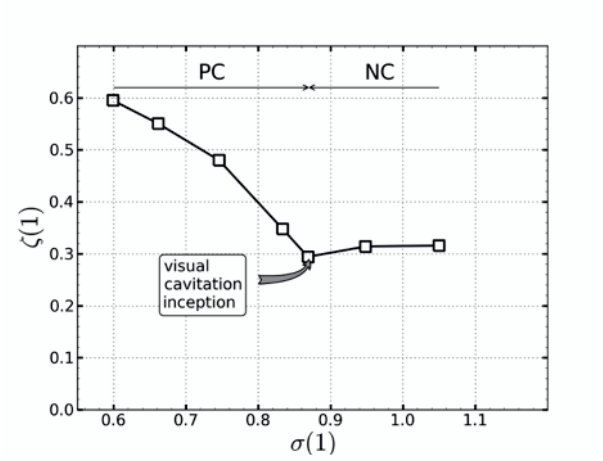

Figure 8. Q = const =5 l/s (NC – no cavitation, PC – partial cavitation)

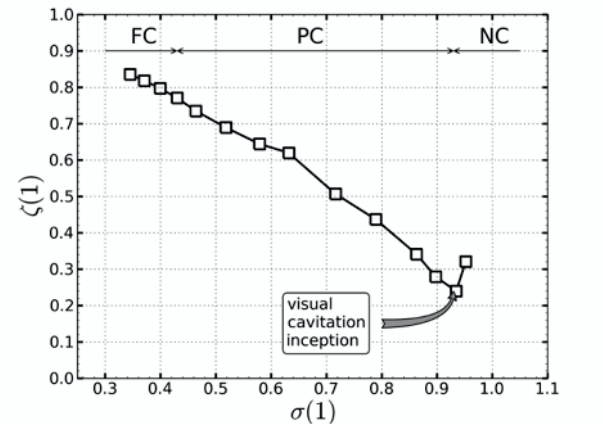

Figure 9. Q = const =6 l/s (NC – no cavitation, PC – partial cavitation, FC- full cavitation)

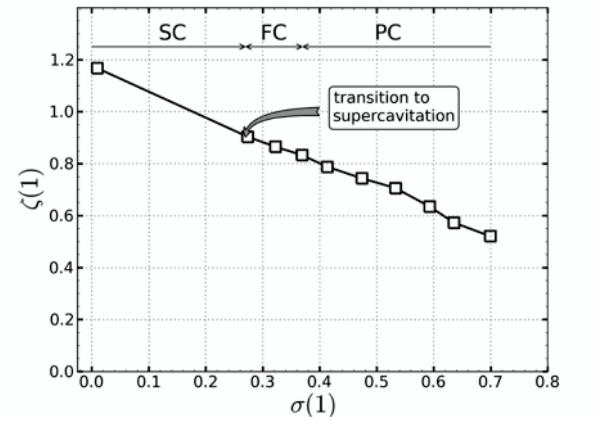

Figure 10. Q = const =7 l/s (PC – partial cavitation, FC- full cavitation, SC - supercavitation)

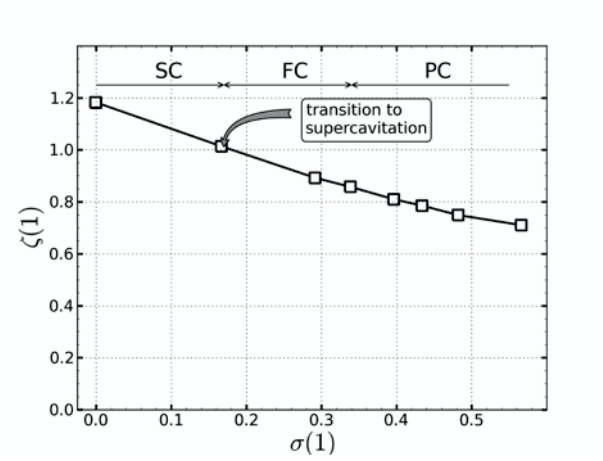

Figure 11. Q = const =8 l/s (PC – partial cavitation, FC- full cavitation, SC - supercavitation)

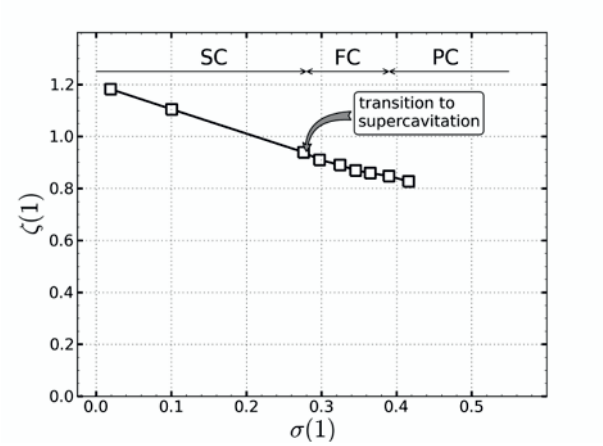

Figure 12. Q = const =9 l/s (PC – partial cavitation, FC- full cavitation, SC - supercavitation)

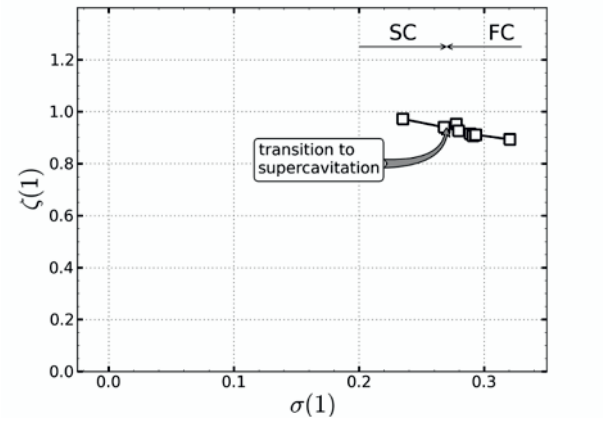

Figure 13. Q = const =10 l/s (FC- full cavitation, SC - supercavitation)

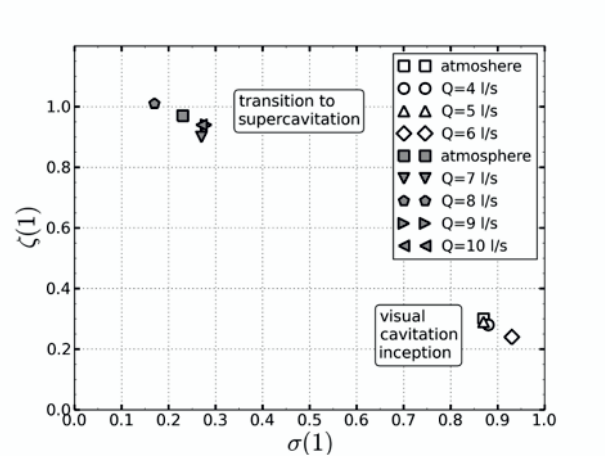

Figure 14. Points of visual cavitation inception and transition to supercavitation for all studied cases

4 Visualization

4.1 Cavitation patterns

Photos were taken for each of the operating regimes to illustrate how is the energy dissipation correlated to the evolution of the cavitation pattern.

4.1.1 No cavitation regime (NC)

Before the onset of the first cavitation bubble are pressure pulsations and acoustic noise low.

4.1.2 Regime of partial cavitation (PC)

Regime of partial cavitation is characterized firstly by appearance of cavitation in the near wall region. Cavitation pattern corresponds to sheet cavitation starting on the sharp edge of the CD nozzle. Decrease of cavitation number leads to separation of the cavitating boundary layers. Vorticity contained within the boundary layer is rolled into vortex ring. It is worth noting that density stratification is additional production term in transport equation of vorticity (so called baroclinic vorticity production).

$$\frac{1}{\rho^2}\mathrm{grad}\rho \times \mathrm{grad}p \qquad (7)$$

Vortex rings travel through the diverging part of the nozzle and then condense.

Vortex rings become more massive with decreasing cavitation number, while their shedding frequency also decreases due to increased compliance of the cavitated region.

Noise level is increased compared to noncavitating regime. Interaction of the vortex ring shedding with the overall dynamic behaviour of the circuit remains yet unclear.

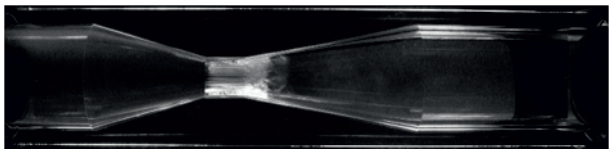

Figure 15. Q = 5 l/s, $\sigma = 0.82$

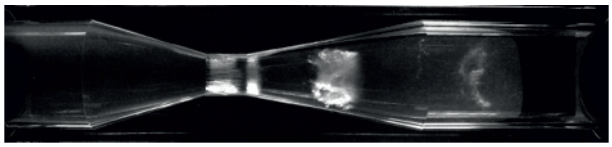

Figure 16. Q = 5 l/s, $\sigma = 0.78$

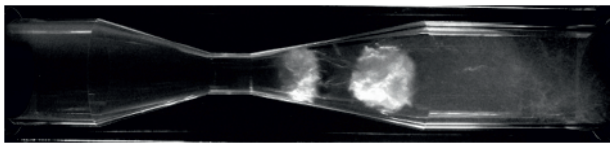

Figure 17. Q = 6 l/s, $\sigma = 0.57$

4.1.3 Regime of fully developed cavitation (FC)

Vortex rings are transformed into huge cavitation clouds with further decrease of cavitation number. Clouds are stretching behind the diverging part of the nozzle and collapse in the rear part of the downstream straight pipe. Fully developed cavitation just prior to transition to supercavitation is characterized by significant increase of the noise level and vibrations of the hydraulic circuit.

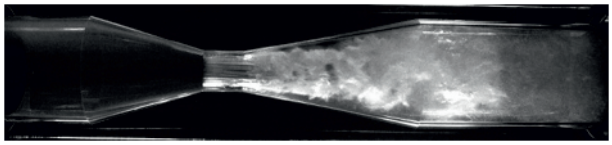

Figure 18. Q = 7 l/s, $\sigma = 0.35$

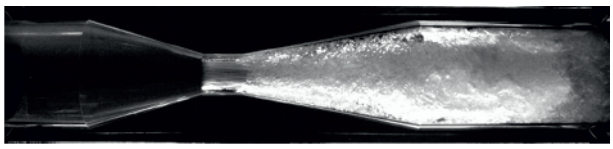

Figure 19. Q = 8.5 l/s, $\sigma = 0.3$

4.1.4 Supercavitation regime

Additional reduction of cavitation number leads to full separation of the boundary layers. Water jet is developed along the axis of the CD nozzle. The jet is surrounded by saturated water vapour, which is confirmed by pressure sensor p_2. Violent condensation of the vapour region occurs in the pressure vessel. Acoustic noise is reduced and flow within the CD nozzle is relatively quiet.

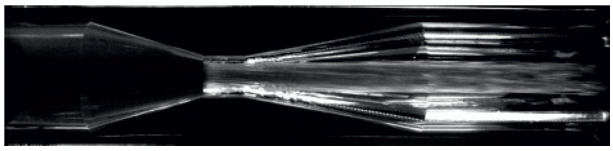

Figure 14. Q = 9 l/s, $\sigma = 0.01$

4.2 Cavitating vortex ring

Vortex rings travelling through the CD nozzle are very interesting phenomenon. Cavitation helps to visualize their shape and behaviour, but also alters their properties. Vortex ring arises from cavitating sheet, which is separating at the rear edge of the CD nozzle throat. The separated vorticity is very quickly rolled into vortex, which is travelling through the diverging part of the nozzle. Flow behind the ring is contaminated by occasional bubbles, which are ejected through the vortex ring center. Sometimes even longer cavitating vortical structures are observed behind the ring, which reminds of the jelly fish tail. No later than vortex ring reaches the end of the diverging part it is weakened and vortex ring undergoes desintegration via undulating instability and then condensation comes.

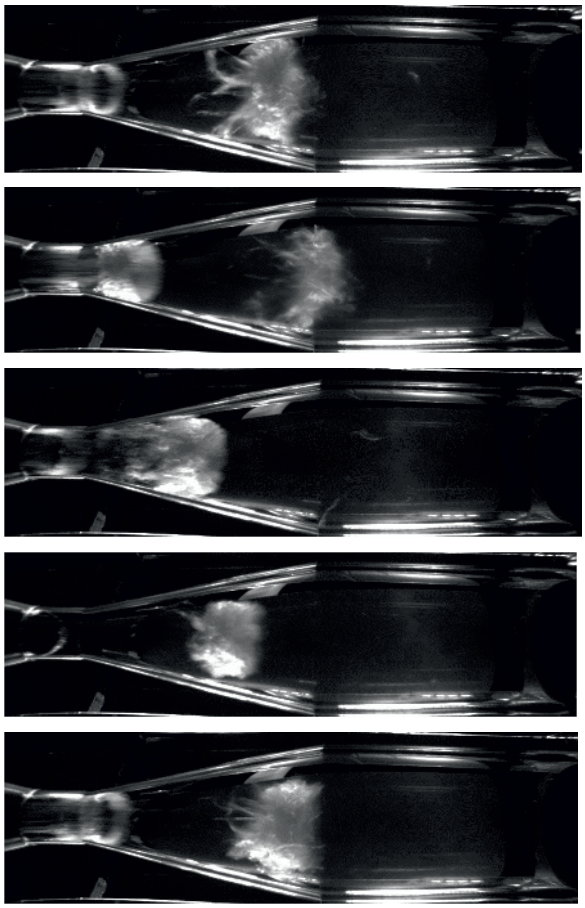

Figure 15. Sequence of photos illustrating evolution of the cavitating vortex ring

5 Conclusion

Experimental observations and measurements confirmed that irreversible energy transformations within converging-diverging nozzle can be correlated with development of cavitation pattern:

- blockage due to cavitation significantly increases hydraulic losses. This increase is uniform from the cavitation inception up to supercavitating regime.
- partial cavitation regime is described by shedding of the cavitating vortex rings. Shedding frequency decreases with decreasing cavitation number.
- most violent regime is the fully developed cavitation prior to transition to supercavitation, which is characterized by substantially increased noise and vibrations.
- supercavitation appears to be relatively stable regime with reduced noise and vibration level.

Further research is focused on quantification of the dynamic behaviour using ultrafast pressure recording and highspeed visualizations.

Acknowledgement

The research has been supported by project of the Czech Science Foundation No P101/13-23550S “Experimental research and mathematical modelling of unsteady phenomena induced by hydrodynamic cavitation” and by project No FSI-S-12-2 “Swirling flow and vortical structures in swirling flow” of Brno University of Technology, Faculty of Mechanical Engineering.

References

1. R.T. Knapp, J.W. Daily, F.G. Hammitt, *Cavitation* (McGraw-Hill, 1970)
2. F.G. Hammitt, *Cavitation and Multiphase Flow Phenomena* (McGraw-Hill, 1980)
3. J.P. Franc, Educational notes RTO-EN-AVT-143 (2006)
4. S. Barre, J. Rolland, G. Boitel, E. Goncalves, R.F. Patella, Eur. J. Mech.-B/Fluids **28**, 3 (2009)
5. J. Decaix, E. Goncalves, Int. Jour. Num. Meth. Fluids **68** (2012)
6. J. Decaix, E. Goncalves, Int. Jour. Heat Fluid Flow (2013)
7. A. Vabre, M. Gmar, D. Lazarro, S. Legoupil, O. Coutier-Delgosha, A. Dazin, W.K. Lee, K. Fezzaa, Nucl. Inst. Meth. Phys. Res. **1** , 607 (2009)
8. M. Dular, I. Khlifa, S. Fuzier, M.A. Maiga, O. Coutier-Delgosha, Exp. Fluids **53** (2012)
9. A.G. Samson, Cavitation in control valves, www.samson.de
10. C.S. Martin, H. Medlarz, D.C. Wiggert, C. Brennen, Jour. Fluids Eng. **103** (1981)
11. A. Osterman, M. Hočevar, B. Širok, M. Dular, Exp. Therm. Fluid Sci. **33** (2009)